PM ENHANCED SENSING OF INTERNAL EMF VARIATION- A TOOL TO STUDY PMBLDC/AC MOTORS

R K Srivastava   S K Singh   Ankita Dwivedi   Srikanth Gollapudi

Dept. of Elec. Engg., I.I.T.(B.H.U.)   Dept of Elec. Engg., V.I.T.
Varanasi (India)   Chennai (India)

Emails: rksrivastava.eee@itbhu.ac.in; sksingh.eee@itbhu.ac.in;
ankitadwd1808@gmail.com ; srikanth.gollapudi.eee10@itbhu.ac.in

Abstract- The search for replacement of commutator and brushes in conventional DC motors by electronic commutator has resulted in a class of Permanent Magnet Brush Less (PMBL) motors. The operation of PMBL motor requires synchronization of coil currents with the instantaneous rotor position. The applied voltages of higher magnitudes must have same zero crossings as that of speed induced back EMF of the respective stator windings. The complexity of rotor position detection in PMBL motor is overcome by obtaining a replica of stator induced EMF using additional auxiliary stator and rotor. The auxiliary stator winding induced EMF is amplified using Power Operational Amplifier (P-OPAMP) and the output is connected to the main stator winding. The proposed scheme has been tested at laboratory scale and has been found to be a promising alternative scheme for operation of PMBLDC/AC motors.

Index terms: Permanent Magnet Brush Less (PMBL) Motors, Power Operational Amplifier (P-OPAMP), PM Enhanced Sensing, Magnetic switch, FEM analysis, Hall Effect sensor & latch.

1. INTRODUCTION

Availability of cost effective and powerful permanent magnets (PM), low loss modern solid state switching devices, Hall-Effect sensors, d-Space and DSP (Digital Signal Processor) / microcontroller have given an impetus to the extensive research and ever growing market of PMBL motors. These motors have higher specific power density, higher torque density and higher efficiency as compared to the conventional motors. They are normally categorized as PMBLDC, PMBLAC (or PMSM), DSPM (Doubly Salient PM) motor etc [1,2,3,4,5,6]. The rotor is in a form of a cylindrical rotor or a disk rotor or a hub-rotor. There are two types of PMBL motors depending on the mounting of rotor PM; Surface Mounted PM (SMPM) and Interior PM Motor (IPM). The SMPM BLDC motor has non-sinusoidal or trapezoidal flux density distribution in space, while in case of IPM motor- the air gap flux density distribution in space is sinusoidal. The PMBL motors with sinusoidal flux density distribution are also referred as Permanent Magnet Synchronous motors (PMSM). In contrast with SMPM, IPM motors are costly and are having natural reluctance starting torque due to magnetic saliency in the rotor. These IPM motors are reported to be suitable for high speed applications and traction applications [2, 7].

Permanent magnets have found their applications in widespread applications. These PM machines have found their applications in computer peripherals (like cooling fans of personal computer, CD/DVD drive etc.), fans, pumps, household and office applications like tape recorder, digital audio tape recorder [1,6], precision surgery [3], EV (Electrical Vehicles like e-bikes,   e-scooters and e-cars), EHV (Electric Hybrid Vehicles) [4,5,8], turret drive for combat vehicle and aircraft [9], electric propulsors for ship and under water vehicles, sub-sea thrusters [8,9], pumps and compressors [10] , micro-generator for smart grid [18], magnetically levitated contact free micro bearings [19] and multi DOF robotic magnetic actuator [20] etc. Moreover the PMBL motors can be used for continuous load, variable load, to-&-fro drives and also for position sensing applications.

1.1 PRINCIPLE OF OPERATION OF PMBL MOTORS

Theoretically, PMBLDC/AC machine is working on the same principle as that of conventional DC machine, except that its commutator is replaced by an electronic commutator. If one considers conventional DC generators connected in parallel to a DC grid, one observes that if the grid

voltage is less than the developed EMF, the machine behaves as generator and when the grid voltage is equal to developed EMF the machine floats on the DC grid. However when the supply voltage is more than the developed EMF the machine works as a motor. It is therefore proposed to operate BLDC/AC motor on the same philosophy. Further, in case of two parallel connected DC shunt machines - used in Hopkinson's Test, the AC induced EMF in a particular coil of first machine has identical zero crossing as that of EMF induced in a similarly disposed coil of the second machine, though the magnitudes of their induced EMF may differ. On the same analogy the controller of PMBLDC/AC motor has been developed. In case of PMBLDC/AC motor, the instant of commutation is important for safeguarding the demagnetization of permanent magnets, better motoring torque and also for mitigating the harmonic contents in the supply current.

PMBLAC motor is similar to an AC synchronous motor with permanent magnet mounted on the rotor and winding on the stator. By using an appropriate sequence of supply to the stator phases a rotating magnetic field on the stator is created and rotor rotates in an attempt to follow the rotating magnetic field. They are also referred as a type of synchronous motor as the stator magnetic field and rotor rotates at same frequency. As has been reported earlier, there are two types of stator winding viz., trapezoidal (SMPM type) and sinusoidal (IPM type) motors. The differentiation is made on the basis of the interconnection of coils in the stator windings to give the different types of back EMF. In addition to the back EMF, the phase current also has trapezoidal or sinusoidal variations in the respective types of motor. This makes the output torque by a sinusoidal motor smoother than that of a trapezoidal motor [11].

Depending on the spatial distribution of windings and resulting no-load EMF waveforms, the PMBL motors can operate in DC or AC modes. For a trapezoidal back-EMF, PMBLDC operates in 120° mode. When the flux linkage 'λ' or speed induced EMF 'e' in a coil increases with the rotor position, a positive armature current is applied with the conduction angle 120° for DC operation and the conduction angle 180° for AC operation. This results in a positive torque. When 'λ' or 'e' decreases with the rotor position, a negative armature current is applied resulting in a positive torque. Thus, the whole cycle of flux linkage is utilized for torque production. PMBLAC operation is known to be superior below base speed, whereas PMBLDC -180° operations is better in flux weakening region [2].

A typical slot star of 12-slot single phase PMBLAC motor is shown in Figure 1. When only half cycle of EMF is utilised the machine can operate in 120° PMBLDC mode with lesser torque. A

typical back-EMF 'e' or flux linkage 'λ' versus time in PMBLDC/AC machine is shown in Figure
2(a). When Hall Effect sensors are in use, the position signal is in synchronism with zero crossing
of the open circuit speed induced EMF of the windings. These typical bipolar Hall sensor and latch
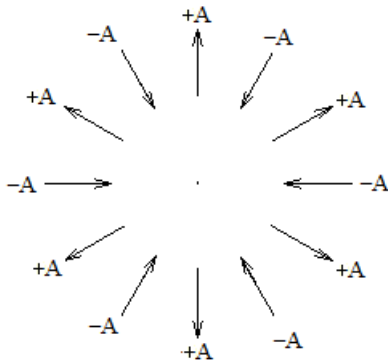signals are shown in Figure 2(b).

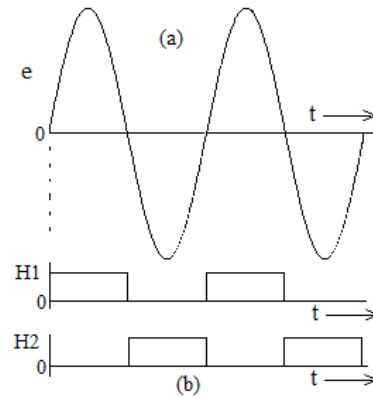Figure 1. Typical slot star of 12 slot single
phase PMBLDC/AC motor

Figure 2. (a) Typical steady state speed induced
EMF 'e' in the stator windings (b) Hall Sensor &
latch outputs corresponding to zero crossing of
EMF induced 'e'

A current chopping scheme can also be utilised in PMBLDC/AC operation which ensures that the
coil current does not rise to a large value when a coil is switched ON. Figure 3(a) shows a typical
circuit using Hall sensor for operating single/two phase PMBLDC/AC motor. The typical voltage
wave forms without current chopping and with current chopping are shown in Figure 3(b) (i) & (ii)
respectively. In uni-polar 2- phase windings, one phase of winding is ON when N pole is in
proximity to it and the second phase of winding in different slot teeth is energized when S pole is
closer to it. Thus the winding currents in both the windings will be uni-directional. Smaller
capacity two-phase machines are having similar winding construction. In case of bifilar windings,
the two parallel conductors are used for making coil, in which one of the terminals is common and
voltages of different polarity are connected to the other two terminals alternatively depending on
the rotor position. The operation is similar to PM stepper motor. Schematic diagrams for unipolar
and bifilar winding are as shown in Figure 4(a) and 4(b) respectively.

For 120° PMBLDC and PMBLAC operations, Hall Effect signals need to be modified as shown in
Figure 5(i) and (ii) respectively. This requires signal conditioning preferably based on the

microcontroller because the frequency of signals varies from zero to maximum during starting period. For 120° and 180° BLAC motor operation, H-bridge is essentially required. At the time of zero crossing of speed induced EMF, there is a possibility that two switches in the same leg of the H-bridge are conducting or ON, thereby short circuiting the power supply. This ultimately results in large short circuit current, which eventually may lead to permanent failure of the power devices. It demands a blanking signal 'V_b' at zero crossing as shown in Figure 5(iii).

2.0 TECHNICAL BACKGROUND

The need for rotor position sensing has been discussed earlier. In sensor/transducer based rotor position detection schemes, the signal corresponding to rotor position is detected using certain sensor / transducer. As far as historical developments are concerned, Yates and Skamfer [12] have reported high frequency reluctance switch for instantaneous rotor position detection. The present day *resolvers* are an extension to the same technique. Bosch [13] has reported Si-Hall-effect chip for instantaneous rotor position detection. The Hall IC efficiently detects the zero flux instant arising out of the armature reaction due to heavy mechanical loading. Majority of the PMBL motors used today employs either Hall-effect sensor or combination of Hall-effect sensor & latch for their working. Tripathi et al. reported the use of search coils in instantaneous rotor position detection [14]. However, due to Hysteresis effect, the search coil signal of instantaneous rotor position deviates from actual signal. Unnewehr et al., have reported the feasibility studies of different types of possible schemes such as optical disk encoder, light actuation of reed switches, permanent magnet enhanced sensing of internal motor reluctance variation [15]. The proposed scheme is an extension of Unnewehr [15] work, where instantaneous rotor position is determined using permanent magnet enhanced sensing of motor EMF variation. The EMF thus obtained is amplified using commercially available P-OPAMP for supplying power to torque producing windings [17,23,24].

The sensing of rotor position is done using Hall Effect sensor, resolvers, use of shaft encoding of different types and also by the rotor position by sensing the variation of electrical quantities in the motor electric circuit. The latter is referred as sensorless control. Initial development and commercialization of PMBL motors were based on rotor position sensing using Hall sensors.
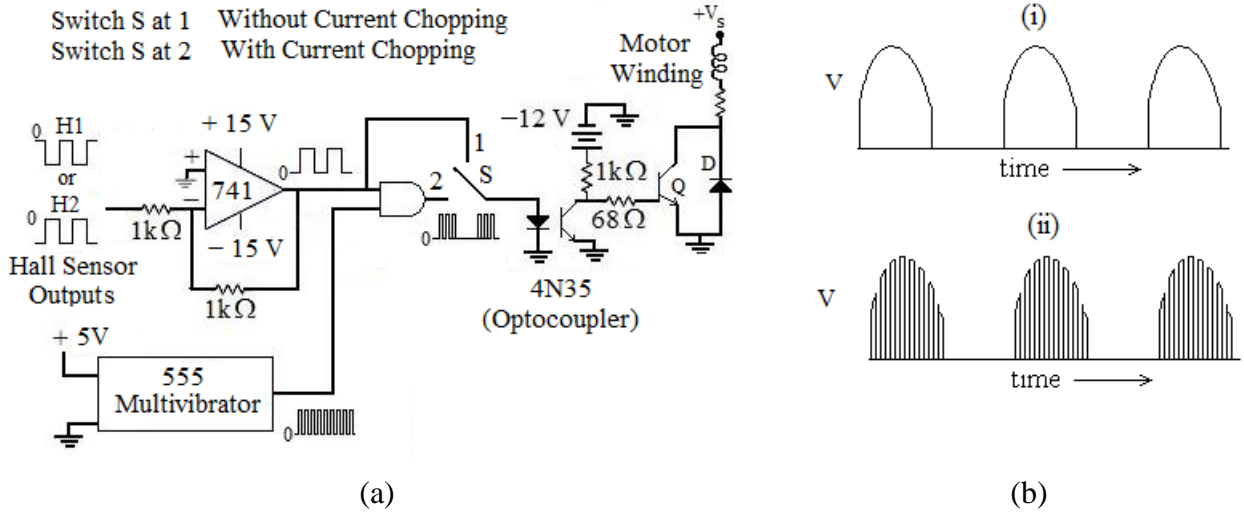
Figure 3(a). Typical Hall sensor scheme for operation of PMBLDC motor (b) Typical voltage wave
forms (i) without current chopping and (ii) with current chopping

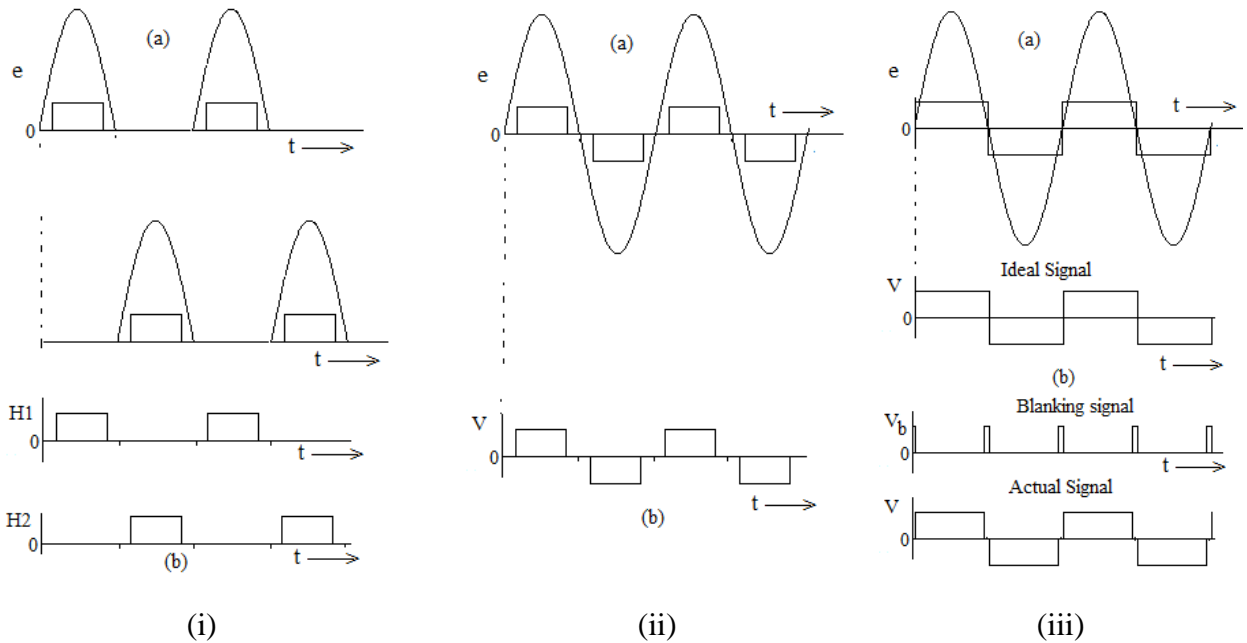Figure 4 (a). Uni-polar windings (b) Bifilar windings

Figure 5 (i).120° PMBLDC; (ii) 120° PMBLAC (iii) 180° PMBLAC operations

When motor is mechanically loaded the voltage and current waveforms are highly complex and distorted. In case of sensorless control, it is quite cumbersome to extract the necessary information of zero crossing of the speed induced back EMF. The instant of commutation of armature coil currents is important for preventing the demagnetization of permanent magnets and also for positive torque production.

The technology of sensorless operation and control of PMBL motors is growing at a faster pace due to availability of powerful cheap electronics, microprocessors, micro-controllers, d-Space and DSP [7, 8, 10, 16]. In sensor less control, it is quite cumbersome to extract the information of zero crossing of the induced back EMF because of complex voltage and current waveforms when machine is working under heavy mechanical load. Sensorless technique is based on the indirect assessment of instantaneous rotor position by on line estimation or real time of instantaneous λ-i (flux linkage and current) or mutual voltage or inductance of coil or observer based waveform detection [7, 8]. Their implementation requires a thorough knowledge of microcontroller, d-Space, DSP (Digital Signal Processing) or FPGA (Field Programmable Gate Array). The sensorless schemes for PMBL motors are not the area of current discussions.
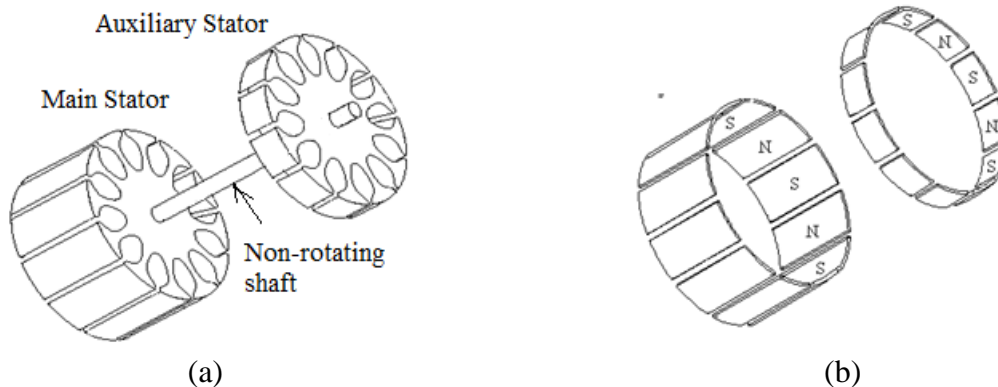

(a) (b)

Figure 6 (a). Twin inner stators-auxiliary and main on common non rotating shaft (*winding is not shown for clarity*) (b) Twin alternate PM arrangements on a common hub outer rotor (*other mechanical part are not shown for clarity*)

The speed induced EMF in the armature coil of field excited or PM excited machine follow the spatial distribution of magnetic flux density distribution in air gap. In case of conventional DC motor or PMBL motor, speed induced EMF in a coil is AC due to rotation of armature coil under the influence of two opposite magnetic poles - *rotational magnetization.* For motoring operation of PMBL motor, the applied AC coil voltage should be in phase and also higher than that of speed

induced AC back EMF in the coil. Any change in the phase difference between applied voltage and instantaneous winding induced EMF results in change in the torque speed characteristics of the brush less motor [17, 25]. For normal motor operation of PMBL motor, the zero crossing of back EMF is regarded as most suitable signal for commutation of coil current. Though, its use in PMBL motor operation has never been reported in the literature. The speed induced back EMF indirectly gives information about the instantaneous rotor position. When solid state switching devices like IGBT or MOSFET are used, it is difficult to estimate the zero crossing instant of speed induced back EMF of a coil because of several switching harmonics. In the present paper, an attempt has been made to obtain the pattern of speed induced back EMF utilizing PM enhanced sensing of internal EMF variations for the operation of PMBLDC/AC motors.

3. PROPOSED SCHEME

The paper proposes an alternative, novel and foolproof scheme of operation of PMBLDC/AC motor which can be used in e-bikes or in applications where the provision of starting torque is not a major consideration. The scheme can also be implemented in fault tolerant PMBLDC/AC motor for reliable operation in the event of failure of primary Hall Effect sensor and / or power circuits. An innovative way is to provide a similar stator of lesser stack length as shown in Figure 6; both the stators are facing similarly disposed alternate permanent magnet (PM) N-S-N-S arrangement on its outer hub rotor. The two stators have identical single phase windings as reported in Figure 1. The stator (referred as "auxiliary stator") has lesser stack length; its windings have rotational induced voltage of lower values than that of other stator (referred "main stator") winding. The auxiliary stator winding is identical to that of the main stator winding. Due to relative movement between inner armature and outer hub rotor, speed induced EMF of different magnitudes but identical zero crossing appears on both the windings. The auxiliary winding back-EMF is amplified using P-OPAMP either L165 or LM675 [21,22]. The side view of the developed prototype is shown in Figure 7(a) and the details of stamping used are depicted in Figure 7(b).The amplified voltage is then connected to the main winding. The schematic diagram of the windings of the proposed scheme is shown in Figure 8(a). The scheme with proposed SCR control & P-OPAMP is given in Figure 8(b).

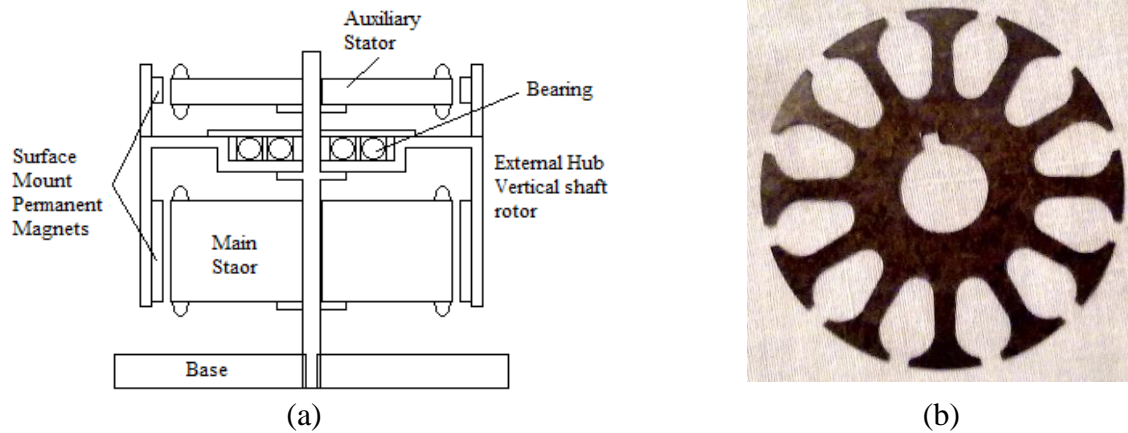(a)   (b)

Figure 7(a). Axial Cut view of the developed machine (b) Details of stamping used

A 12-slot experimental vertical shaft hub rotor PMBLDC/AC motor with auxiliary and main armature facing identical alternate permanent magnet structure on the rotor has been developed. The inner stator has a common non rotating shaft which supports the outer hub rotor. Ferrite strip magnets of 0.3 T have been used on the hub rotor. There are twelve coils in each of the stator and each coil is having 165 turns of S.W.G. 32 [17]. The auxiliary induced EMF is amplified using P-OPAMP, the amplified voltage is then connected to the main stator windings. As mentioned earlier, the circuit uses either L165 or LM675 P-OPAMP for voltage amplification. The level of output voltage can be suitably increased by adjusting the gain of amplifier and biasing voltage.

At no-load, the EMF induced in the auxiliary winding is truly a replica of EMF induced in the main winding. This scheme of PMBLDC/AC motor operation does not precisely require rotor position estimation. The details of the prototype are given in APPENDIX-A. Similar construction of outer stator and inner rotor with rotating shaft is possible as shown in Figure 9 [23, 24].

3.1 USE OF POWER OPAMP IN PMBL MOTOR

The operational amplifiers such as 741 series are meant for changing the signal level/voltage that are having current rating of about few mA. These are not suitable for working at higher currents. For example, a Wien-bridge oscillator based on 741 IC at 400 Hz cannot cater to a load curren of 3.0 A. The P-OPAMP have been widely used in aicraft /space craft power supply of 400Hz and higher. These industrial power devices can sustain up to a load current of more than
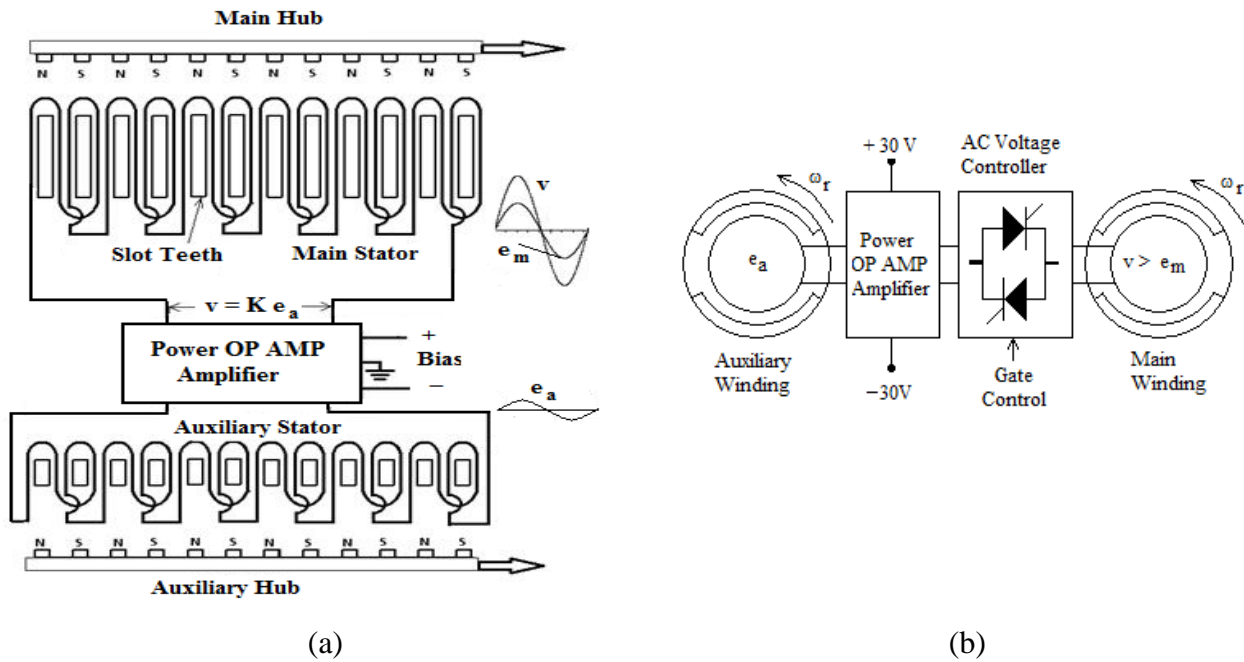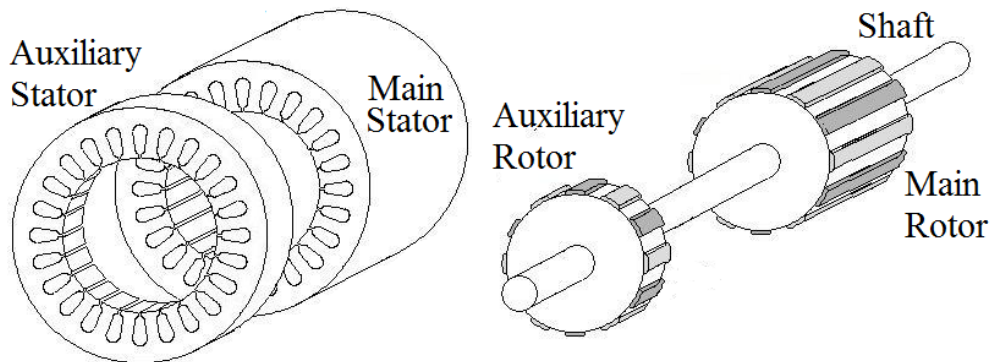
(a) (b)

Figure 8 (a). Schematic winding and circuit diagram of set up for single phase PM enhanced sensing in a 12 slot PMBLAC motor (b) Schematic Diagram for BLAC motor using PM enhanced sensing of rotor internal EMF with AC voltage controller [17]

(a) Twin stators-auxiliary and main (b)Twin alternate PM rotor on rotating shaft

Figure 9. Outer Stator and Inner rotor arrangement of the proposed scheme (*other mechanical parts and windings are not shown for clarity*)

40 A at different voltage levels. The industrial P-OPAMP has voltage ratings 100V-500 V and current ratings 1.5-40 A. The present study is reported on the basis of experience gained with Texas Instruments LM675 and ST Micro-electronics L165. The other available P-OPAMP which can be utilized for developing similar large size motors are LH0101, LM12, etc.. The present paper discusses the use of L165 [21] and LM675 [22] in PM enhanced sensing. The P-OPAMP circuits

for L165 and LM675 are shown in Figure 10(a) & (b) respectively. The following subsections deals with the studies of PMBLDC motor using the above two P-OPAMP. Typical safety measures are: Bias voltage should not be more than rated bias voltage; Use of an efficient heat sinkis efficient; Positive and negative bias voltage should be identical. The scheme does not require additional power supplies as is common in case of sensor control of PMBL motor. The scheme is very simple and straightforward. The applied voltage is almost sinusoidal voltage free from harmonics.   However due to trapezoidal flux density distribution in air gap, the input current contains odd number of harmonics.

The speed control of the developed motor is possible by either changing the bias voltage/voltage amplification of P-OPAMP or by changing the firing angle of AC voltage controller. In the present scheme, the chances of under-commutation or over commutation are remote. The scheme reported with P-OPAMP does not require solid state power switching devices like MOSFET or IGBT based PWM inverter. The auxiliary winding EMF may also be used for developing IGBT/MOSFET based single switch or H-bridge control circuit DC/AC operations of PMBL motors.

The air gap flux is trapezoidal due to mounting of strip magnets, it can be assumed to vary co-sinusoidally. As reported earlier, the control of phase angle between main and auxiliary winding EMF results in modifications in the torque speed characteristics of machines. In the present set up, it is possible to create a phase difference between applied voltage and the EMF induced in main winding by two means. First, a slight variation in the alignment of either main winding or auxiliary winding with respect to the perfectly aligned rotors results in a phase difference. Second method includes the electronic correction using the OP AMP circuit. Several similar P-OPAMP circuits can be used in case of multi-phase PMBLDC/AC motors and also in fault- tolerant motors.

3.2 EFFECT OF ARMATURE REACTION IN PMBL MOTOR

In conventional DC motors, the armature rotates inside while the outside field is stationary. In the present test motor, the inverted structure has been use to check the feasibility of the proposed scheme. In these motors, the rotors will essentially carry PM. As has been mentioned earlier, the scheme is suitable both for outer stator and inner rotor and vice versa, and can be made for different number of poles and phases. The Magnetic Neutral Axis (MNA) in conventional DC

(a)   (b)
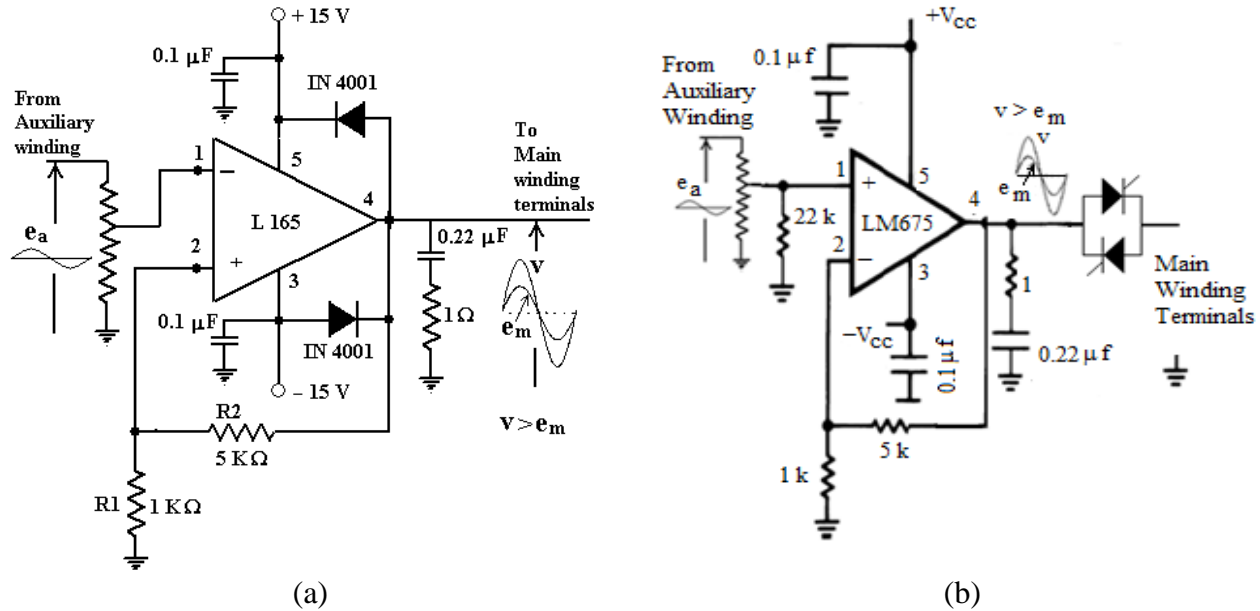
Figure 10 (a). Power Operation amplifier circuit using L165 P-OPAMP for driving PMBLAC motor (firing circuit not shown for clarity) (b)   Power Operation amplifier circuit using LM675 P-OPAMP for driving PMBLAC motor (firing circuit not shown for clarity) [17,21,22]

motor shifts in the direction opposite to that of motor but in present case, the MNA is expected to shift in the direction of rotation. Suppose, a two pole DC motor is running at 1000 RPM, an identical PMBLDC motor due to availability of high power magnets will have lesser diamater giving a comparatively lesser peripheral speed. The shifting of MNA in identical PMBLAC motor will be least as compared to identical conventional DC motor. The effect of armature reaction will be more on main winding, whereas auxiliary winding has no net effect. Since auxiliary winding is not loaded, it does not produce any counter torque. Further, due to armature reaction, there is a possibility of the deteroration of main torque due to difference between zero crossing of applied (amplified auxiliary speed induced EMF) voltage and speed induced EMF of the main winding.

A linear model of PMBL motor is shown in Figure 11(a) with intermediate iron pieces between two poles of opposing polarity N-S acting as magnetic switch. The technique is widely used in commercially available PMBL motors. When conventional stampings are in use, the trend is to provide one slot teeth vacant between two nearby winding phases. The presence of additional iron piece between two opposite permanent magnets forces the magnetic flux linkage to zero when intermediate iron piece and slot teeth are aligned. It is assumed that the rotor is travelling in x-direction with constant linear speed 'v'. Under ideal no-load operation- the zero crossing of flux lies in between two PM. But upon loading the MNA shifts as such there is a shift in zero crossing

of EMF induced in the coil. Figure 11(b) depicts the flux density distribution in space when motor is running without and with magnetic switch, computed using FEM software ANSYS Multiphysics 11.0. In case of magnetic switch, the flux density for two cases approaches zero. This emphasizes the need of providing magnetic switch in design of such types of motor.
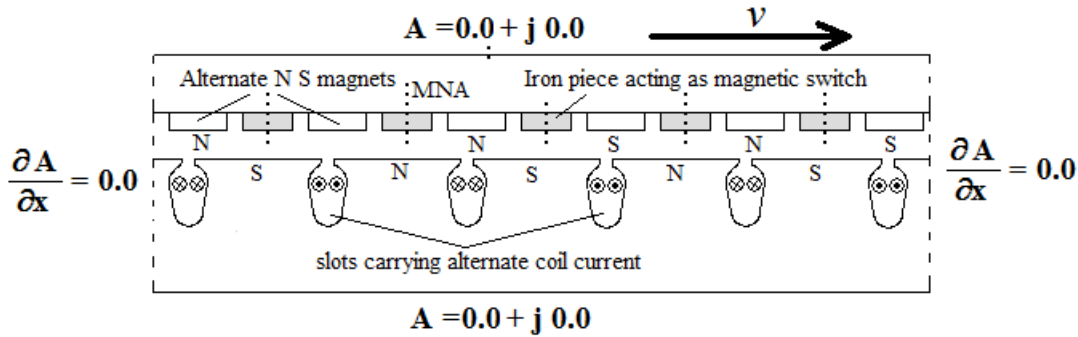

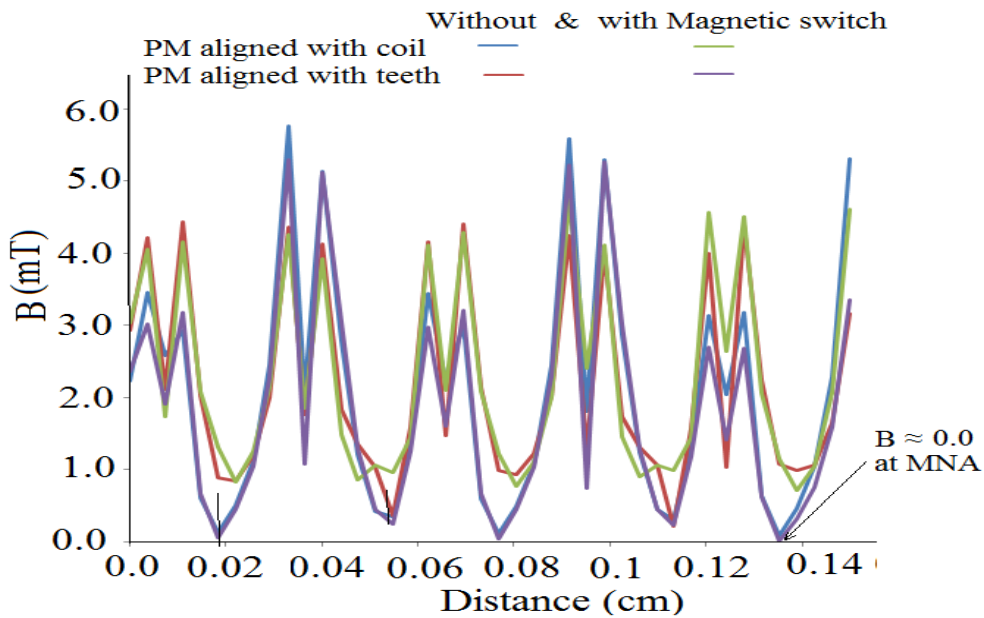Figure 11(a). PMBLDC motor-linear FEM model *(not to the scale)*

Figure 11(b). Total flux density distribution in air gap in presence of velocity without and with magnetic switch computed using FEM software ANSYS Multiphysics 11.0

The windings in BLDC/BLAC operations may be multi-phase although the coil orientation may be unipolar, bipolar or even distributed windings. The PM enhanced sensing of the internal induced EMF variation can be used to study the 120° BLDC/BLAC operations and 180° multi-phase BLDC/BLAC operations. Schmitt trigger may be used to obtain the nearly 120° operation of the

PMBL motor. This avoids the use of microcontroller. As has been mentioned earlier, it is also suitable for fault- tolerant and multi-phase PMBL motors. The typical winding arrangement for fault-tolerant and multi-phase motors [23, 24] is shown in Figure 12. However the disposition of PM also differs in both the schemes. One can visualize rotor having four, six, eight pole construction with these windings.

(a) Scheme -I   (b) Scheme-II

Figure 12. Winding divided into different phases

4. RESULTS

The developed motor was initially operated with Hall sensor and a uni-polar transistorized latch circuit and was found to work satisfactorily at 30V DC. Typical Unipolar Control of PMBLDC motor using Hall sensor and IGBT-without current chopping is shown in Figure 13. A P-OPAMP L165 with bias voltage of ±15V was initially used to study the feasibility of such scheme [21]. The aim of the current work is to replace Hall-effect sensor and sensorless control by some suitable rotor position sensing scheme. The feasibility of the proposed PM enhanced sensing of rotor internal EMF has been investigated. The air gap of the motor is decreased by pasting an extra layer of strip magnets. When again excited with similar scheme of L165, the bias supply capable of giving 1.0A was found to be overloaded. As a consequence of lesser air gap, the speed induced in coils has increased for the same velocity. The scheme could be made operational using Texas instruments P-OPAMP LM675 having bias voltage of ±30V. The LM675 is a Monolithic P-OPAMP featuring wide bandwidth and low input offset voltage, making it equally suitable for AC and DC applications [22]. The LM675 is capable of delivering output current in excess of 3.0 A, operating at supply voltage of up to 60V. The device overload protection consists of both internal current limiting and thermal shutdown. The amplifier is also internally compensated for gains of 10 or greater. Figure 14 shows the typical Magnetic Vector Potential (MVP) in and around the geometry of the machine which has been computed using commercially available FEM code ANSYS Multiphysics 11.0.
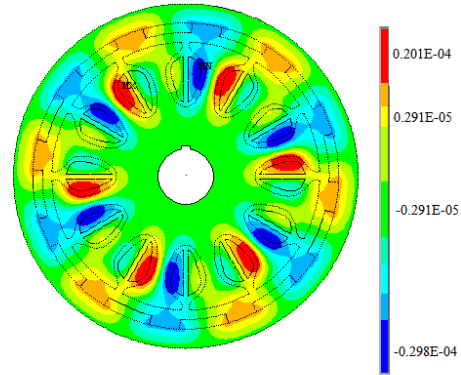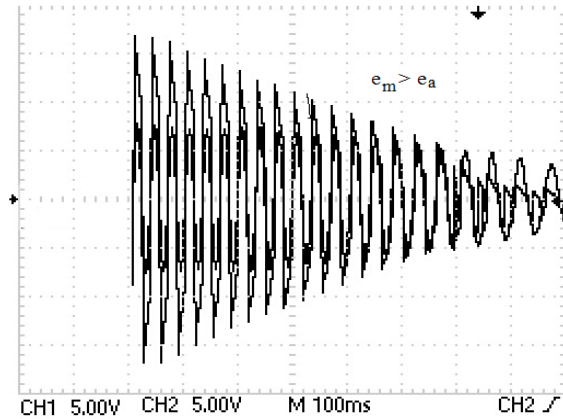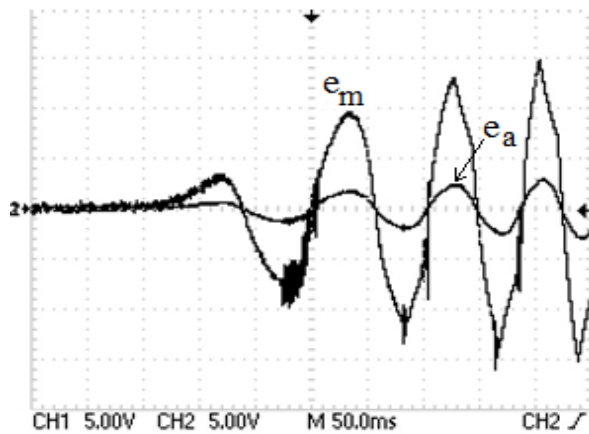
Figure 13. Typical Unipolar Control of PMBLDC motor using Hall sensor and IGBT-without current chopping

Figure 14. A typical Magnetic Vector Potential computed using ANSYS 11.0

(a) Start up   (b) Halt

Figure 15. Auxiliary winding voltage and main winding voltage waveforms

The voltage waveforms of main and auxiliary windings during start up and halt are shown in Figure 15 (a) and (b) respectively. Due to use of flat strip magnets and saturation in P-OPAMP, the voltage waveform is not exactly sinusoidal and it also contains some high frequency components during starting with L165. Figure 16(a) shows the no-load steady state auxiliary and main winding voltage waveforms, when the rotor is allowed to move due to external starting torque. In the event of frictional loading of rotating outer hub, the waveforms of main and auxiliary winding voltages are shown in Figure 16(b); it results in slight reduction in the speed of the machine. In all these waveforms, $|e_m| > |e_a|$, as has been discussed in APPENDIX-B. Here, the saturation in P-OPAMP and presence of cogging torque both result in non sinusoidal voltage on the main winding terminals.
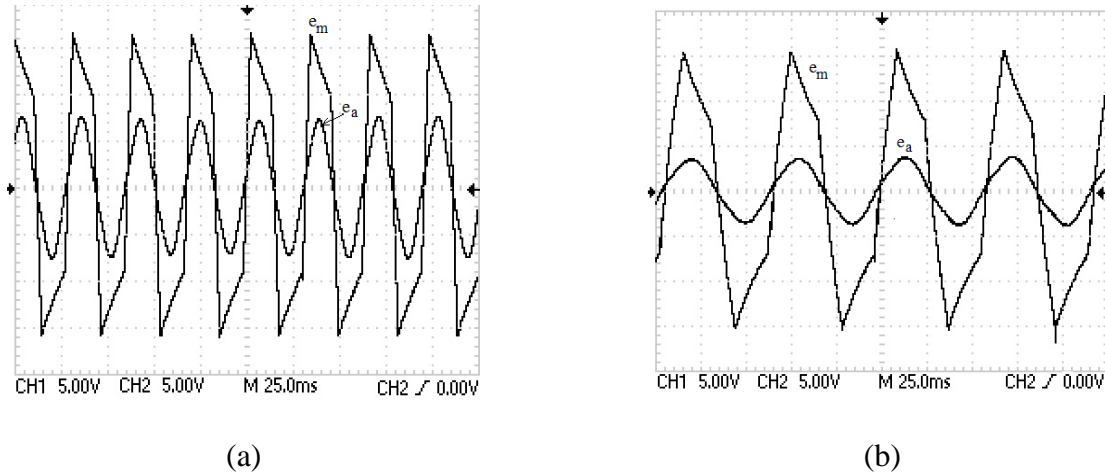
(a)   (b)

Figure 16. Auxiliary winding voltage (e_a) and main winding voltage (e_m) waveforms of developed prototype with L 165 at (a) No-load (b) Load

Similar waveforms with LM675 have been reported earlier [17]. These are given in Figure 17 and 18. Here one can visualize that the effect of cogging torque is less on the voltage waveforms.
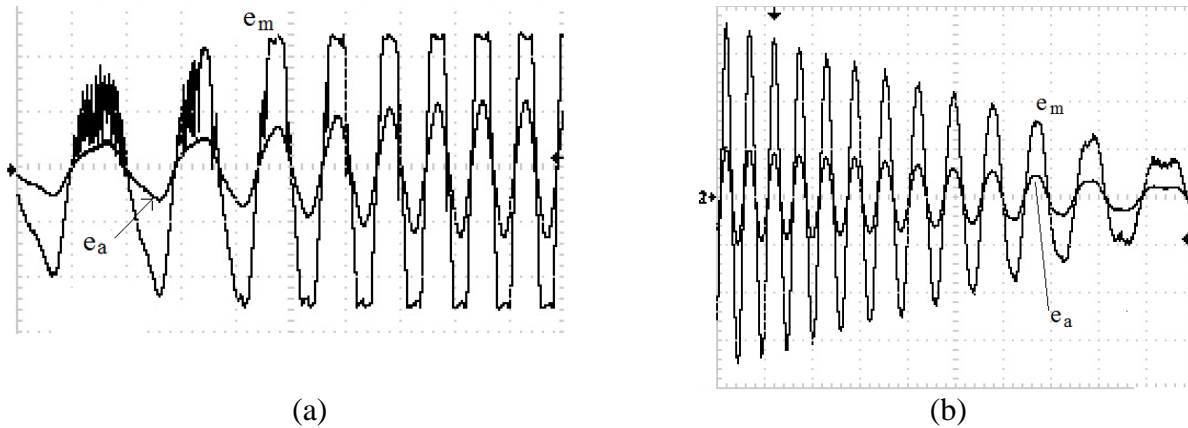

(a)   (b)

Figure 17 (a). Starting transient voltages main winding and auxiliary winding at bias voltage ±30V *(Scale 10V/div and 5.0 V/div; 50 ms /div)* (b) During halt with LM675 *(Scale 5V/div and 5.0 V/div; 100 ms /div)* [17]

The torque- speed characteristics obtained [17] for the test motor upon loading is shown in Figure 19(a). The theoretical results have been calculated using Ref [25] given in APPENDIX-C and the compared with the experimental results. It can be observed that experimental results validate the theoretical results.
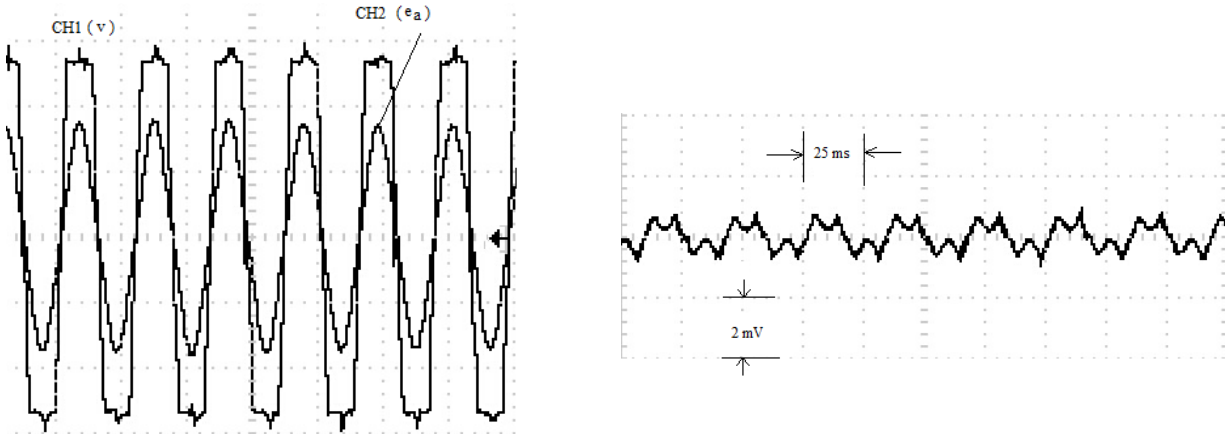
Figure 18 (a). Voltage waveforms across main and auxiliary windings for steady state operation with LM675 *(CH1 10 V/div, CH2 5 V/div, 25 ms/div)* Bias ±30V (b) Typical steady state current waveform at no load measured across a resistance of 1.0 Ω connected in series with main winding *(2mV/div, 25 ms /div)*[17]

The torque-speed characteristics of the prototype motor with different magnets are depicted in Figure 19(b). These characteristics are likely to improve with higher torque at low speed, when Nd-Fe-B magnets are in use. However for high speed operation the flux weakening with ferrite magnets is a better choice.
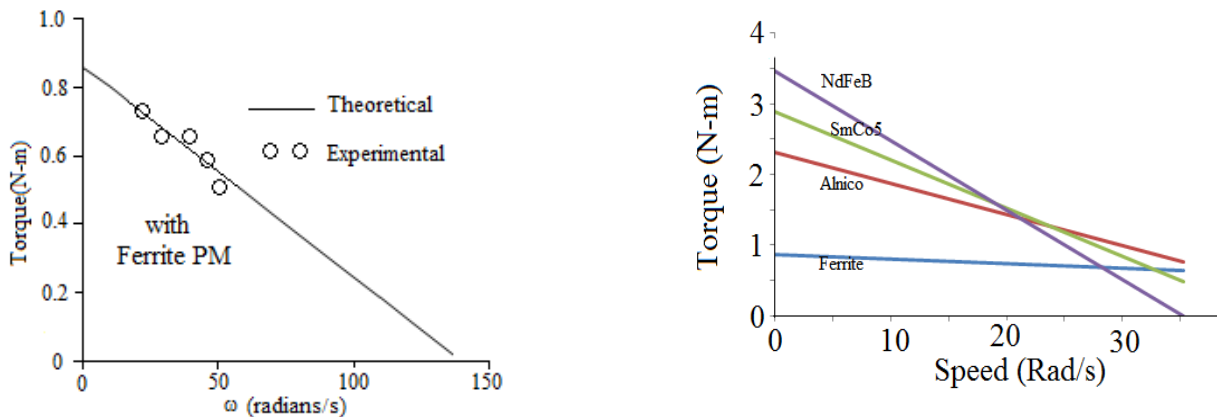

Figure 19 (a). Comparison of theoretical and experimental torque speed characteristics (b) Effect of changing type of magnets

It has been mentioned earlier that initially the air-gap in the developed motor was 3.0 mm (similar to flux weakening condition). Extra layer of magnets were pasted over the existing magnets, thereby reducing air gap to 1.0 mm. The effect of air gap or change of magnetic flux is depicted in Figure 20.
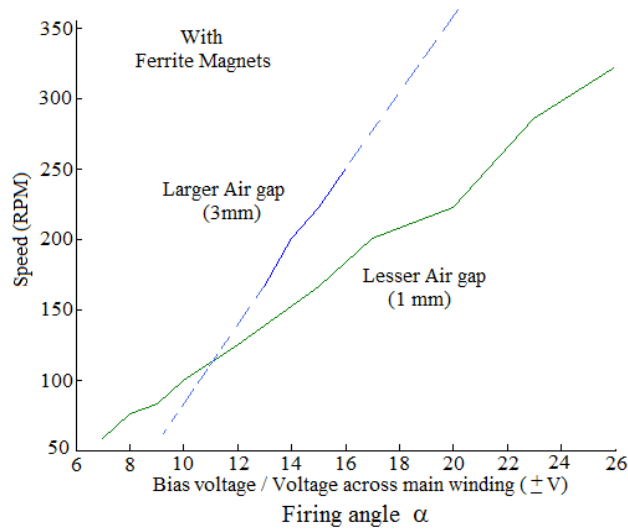
Figure 20. Variation of no load speed with respect to bias voltage and firing angel of AC voltage controller.

4.1 ISSUES WITH THE PROTOTYPE MOTOR

The fabricated 12 slot, 12-pole single phase PMBLAC motor is not self-starting. PMBLDC motors resembles an AC induction motor wherein the supply frequency is gradually increasing. The natural starting torque in case of PMBL DC motor can be made available by providing multi-phase (two phase and above) winding. In case of shaded pole motor, the natural torque is obtained by shifting the phases of the flux. In PMBLDC motor if the PM flux is impinging the stator slot teeth normally, it will not cause a net starting torque-a condition resulting in cogging torque. But if the PM flux is made to imping the the teeth surface at an angle other than normal, the natural starting torque can be expected. The use of Chirp voltage with rising voltage magnitude and frequency both during starting may result in self starting.

4.2 COMPARISON OF SENSING METHODS BY HALL SENSOR H- BRIDGE METHOD & PM ENHANCED SENSING METHOD IN PMBL MOTORS

Number of isolated power supplies needed are large in Hall sensor & latch H-Bridge method, while in PM enhanced sensing single power supply is needed inspite of large number of phases and number of P-OPAMPs used; Harmonics in the current and voltage will be more in case of PWM

H-bridge Hall sensor scheme as that of PM enhanced sensing method thereby giving better efficiency in the latter case; Signal conditioning circuit is necessary in H- bridge, while it is not required in present case; Hall sensor based H-bridge is likely to have problems when motor works in vibration prone area but because of rigid construction in case of PM enhanced sensing it is better; Additional PCB's is mounted on the stator with Hall IC sensor, but in present case overall axial length is slightly increased. Moreover, it is possible the scale down the size of auxiliary stator and rotor such that an increase in axial length can be optimized.

It has been pointed out earlier that the scheme is also suitable used in multi-phase brushless motors and fault tolerant BLDC/AC motors [23,24]. A typical schematic diagram for such motors is shown in Figure 21.
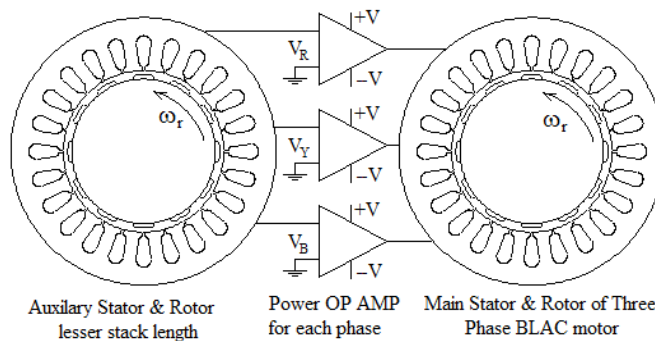

Figure 21. Proposed scheme for Multi-phase BLDC motor

In absence of proper biasing of P-OPAMP and over current in the load circuit etc. causes major failure of P-OPAMP circuit which may disrupt the operation of PMBLAC motor. Design of robust bias power supply for supplying ±30V with 3A capacity is highly required.

5. CONCLUSIONS

The proposed scheme of PM enhanced sensing for Brushless motors is tested for single-phase brushless motors. The feasibility of such scheme for operation of PMBLDC/AC motors have been experimentally investigated and was found that the scheme is suitable for cases where starting torque is provided externally. The need of magnetic switch in designing BLDC/AC motors have been explained. The major draw back of the scheme of starting torque is being tackled by providing chirp voltage in which applied voltage and frequency both are slowly varying. The scheme is suitable in applications like e-bikes, e-trolley, e-scooters etc. In large vehicles a pony

drive may serve the purpose of starting motor in one direction. Bi-directional operation are possible. The scheme proved out to be a very promising in terms of reliability, cost and maintenance. Unlike sensor control of PMBLAC motor, the PM enhanced sensing does not require larger signal conditioning. For multiphase and fault tolerant motors these scheme are being further investigated.

ACKNOWLEDGMENTS

REFERENCES

[1] J.R. Hendershot and T.J.E. Miller, "Design of Brushless permanent magnet motors", Magna Physics Publishing and Clarendon Press, Oxford, 1994

[2] P. Pillay, R. Krishnan, "Application Characteristics of permanent magnet synchronous and brushless DC motors and servo drives", IEEE Trans. on Ind. Appl., 27, (5), Sept/Oct 1991, pp. 986-996

[3] F. Herrault, P. Galle, M. G. Allen, "High speed axial flux permanent magnet micro motors with Electroplated windings", Solid-State Sensors, Actuators, and Microsystems Workshop, South Carolina, June 6-10, 2010, pp. 404-407

[4] Z. Q. Zhu, Y. F. Shi, D. Howe, "Comparison of torque-speed characteristics of interior-magnet machines in brushless AC and DC modes for EV/HEV applications", Journal of Asian Electric Vehicles, 4, (1), June 2006, pp. 843-850

[5] K. T. Chau, C. C. Chan, C. Liu, "Overview of Permanent Magnet Brushless Drives for Electric and Hybrid Electric Vehicles", IEEE Trans. on Ind. Electron., 55, (6), June 2008, pp. 2246-2257

[6] H. Moradi, E. Afjei, F. Faghihi, "FEM Analysis for a Novel configuration of Brushless DC motor without Permanent Magnet", Progress in Electromagnetics Research (PIER) 98, 2009, pp. 407-423

[7] T. Kim, H. W. Lee & M. Ehsani, "Position Sensorless Brushless DC motor/generator drives: review and future trends", IET, Electrical Power Appl., 2007, 1, (4), pp. 557-564

[8] M. F. Hsieh, H. J. Liao, "A wide speed range sensorless control technique of brushless DC motors for electric Propulsions ", Journal of Marine Science and Technology, 18, (5), 2010, pp. 735-745.

[9] P. Snary, B. Bhangu, C.M. Bngham, D. A. Stone, N. Schofield: "Matrix converters for sensorless control of PMSMs and other auxiliaries on deep sea ROVs", IEE Proc. EPA, 152, (2), March 2005, pp- 382-392

[10] J. R. Smith, D. M. Grant, A. A. Mashgari, R.D. Slater, "Operation of Sub-sea Electrical submersible pumps supplied over extended length cable systems", IEE Proc. EPA, 147, (6) , Nov 2000, pp. 544-552

[11] P Yedamale, "Microchip AN885 Brushless DC (BLDC) Motor Fundamentals", Microchip Inc. Technology, DS00885A-page 1- page 20, 2003.

[12] W. W. Yates and R.E. Skamfer, "A new brushless D-C torque motor system with integrated controller", Supplements on the IEEE Trans. on Aerospace and Electron. syst., AES-2, 4, July 1966, pp. 116- 124

[13] G. Bosch, "A Switching Circuit for a Brushless DC Motor Containing an integrated Si Hall Element", IEEE Int. Solid-state Circuits Conf., Univ. of Pennsylvania, Feb. 20,1969, pp. 112-113

[14] K.C. Tripathi , P. Lal, P.R. Sharma, A. N. Sharma and V. Prakash, "A Battery-Run Pulsed Motor with inherent Dynamic Electronic Switch Control", IEEE Trans. on Ind. Electron. and Control Instr., IECI-27 (1), Feb 1980, pp. 29-34

[15] L.E. Unnewehr, P. Piatkowski and D. Giardini, "A Brushless DC motor for Vehicular AC/Heater application", 26th IEEE Veh. Technol. Conf., March 1976, pp. 8-15

[16] G.H. Jang, J.H. Park , J.H. Chang, "Position detection and start-up algorithm of a rotor in a sensorless PMBLDC motor utilizing Inductance Variation", Proc. IEE Electric Power Appl., 149, (2), March 2002, pp. 137- 142

[17] R. K. Srivastava, S. K. Singh, S.K., A. Dwivedi, and S. Gollapudi, "Operation of Single phase BLAC Motor Using PM Enhanced Sensing of Internal EMF Variation", 6th International Conference on Sensing Technology (ICST 2012), India, December 18-21, 2012, pp. 336-340 (available in IEEE Xplore)

[18] Adel El Shahat, Ali Keyhani and Hamed El Shewy, "Micro-Generator Design For Smart Grid System (Comparative Study)", International Journal On Smart Sensing And Intelligent Systems, Vol. 3, No. 2, June 2010, pp-176-216

[19] T. Nakao, H. Han, And Y. Koshimoto, "Fundamental Study Of Magnetically Levitated Contact-Free Micro-Bearing For MEMS Applications", International Journal On Smart Sensing and Intelligent Systems, Vol. 3, No. 3, September 2010, pp 536-549

[20] Li Zheng, "Neural Network Based Multisensor Fusion In A Novel Permanent Magnet Multi-DOF Actuator Orientation Detection System International Journal On Smart Sensing And Intelligent Systems, Vol. 5, No. 4, December 2012, pp-911-927

[21] Data sheet of L 165, SGS-THOMSON Microelectronics Australia.

[22] Data sheet of LM675, Texas Instruments, Texas.

[23] A. Dwivedi, S. K. Singh and R. K. Srivastava, "Feasibility Study Of Fault Tolerant BLAC Motor Using PM Enhanced Sensing", TIIEC 2013, Bangalore, India, April 4-5, 2013 (presented), to be available in IEEE Xplore by Dec 2013

[24] A. Dwivedi, S. K. Singh and R.K. Srivastava, "Operation of Three phase BLAC Motor Using PM Enhanced Sensing", CERA 2013, Roorkee, India, Nov. 2013 (communicated)

[25] P.C. Krause, O.Wasyncznuk and S.D. Sudhoff, "Analysis of Electric machinery", IEEE Press, New York, 1994

APPENDIX-A

Details of the Prototype Motor:

Items	Main winding	Auxiliary winding
Stator diameter	5.7 cm	5.7 cm
Stack length	4.7 cm	0.8 cm
No. of Slots / Slot area	12 / 79.5 sq mm	12 / 79.5 sq mm
Conductors/slot	330	140
Clearance	1 mm	3 mm
Magnets on Hub rotor	12	12
Magnet Type / Strength	Ferrite / 0.3 T	Ferrite / 0.3 T
Shaft	Vertical	Vertical
Winding resistance / Inductance	40 Ω / 9.55 h	6.8 Ω / 1.62 h
EMF constant	0.302 V/rad/sec	0.151 V/rad/sec
S.W.G. No /No. of coils	32 /12	32 /12
Size of magnet	2.54 x 1.0 x 0.2 cu. cm	2.54 x 1.0 x 0.2 cu. cm

APPENDIX-B

Under steady state condition the speed induced EMF in auxiliary and main windings are,

$$e_a = C_a \omega_r \, sin \, \theta_r$$

$$e_m = C_m \omega_r \, sin \, \theta_r$$

1477

Here C_a and C_m are the EMF constant in Volt/ radian /sec of auxiliary and main winding respectively.

Here angle $\theta_r = \omega_r t$ is the instantaneous angular position of rotor in electrical radians. In SMPM PMBLAC motor $L_d = L_q = L$. The applied voltage to the main windings is,

$$v = Ke_a = KC_a \omega_r \sin\theta_r$$

The circuit equation for main winding is $v = Ri_m + L\dfrac{d}{dt}i_m + e_m$

The developed electromagnetic torque is

$$T_e(t) = e_m i_m \omega_r$$

$$T_e(t) - T_L = J\frac{d}{dt}\omega_r + B\omega_r$$

These set of equations exhibit the operation of proposed PMBLAC motor operation in general and can be solved using 3rd order Runge-Kutta method or MATLAB SIMULINK.

APPENDIX-C

The steady-state characteristics of the PMBLDC motor can be obtained by using following equations [25],

$$V_{qs} = Rsi_{qs} + \omega_r L_d i_{ds} + \omega_r \lambda_m$$

$$V_{ds} = Rsi_{ds} - \omega_r L_q i_{qs}$$

Here λ_m is always constant. Now if assume $L_d = L_q = L$, then the torque equation will become,

$$T_e = \left(\frac{3}{2}\right)\left(\frac{P}{2}\right)\left[\lambda_m i_{qs}\right]$$